

Homogeneous earthquake catalogue for Northeast region of India using robust statistical approaches

Auchitya Kumar Pandey, Prasanta Chingtham & P. N. S. Roy

To cite this article: Auchitya Kumar Pandey, Prasanta Chingtham & P. N. S. Roy (2017): Homogeneous earthquake catalogue for Northeast region of India using robust statistical approaches, Geomatics, Natural Hazards and Risk, DOI: [10.1080/19475705.2017.1345794](https://doi.org/10.1080/19475705.2017.1345794)

To link to this article: <http://dx.doi.org/10.1080/19475705.2017.1345794>



© 2017 The Author(s). Published by Informa UK Limited, trading as Taylor & Francis Group



[View supplementary material](#)



Published online: 07 Jul 2017.



[Submit your article to this journal](#)



Article views: 157



[View related articles](#)



[View Crossmark data](#)

Homogeneous earthquake catalogue for Northeast region of India using robust statistical approaches

Auchitya Kumar Pandey^a, Prasanta Chingtham^b and P. N. S. Roy^{a,c}

^aDepartment of Applied Geophysics, Indian Institute of Technology (Indian School of Mines), Dhanbad, India;

^bNational Center for Seismology, Ministry of Earth Sciences, New Delhi, India; ^cThe Abdus Salam International Centre for Theoretical Physics, Trieste, Italy

ABSTRACT

Regular seismic hazard assessment requires essentially an updated and refined homogenous earthquake catalogue for the study region. Here, we have compiled the earthquake data for Northeast region of India in a chronological order from International Seismological Centre and Global Centroid Moment Tensor databases during the period 1 January 1900 to 31 April 2016. For this purpose, the regression techniques such as least square (SR), inverse least square (ISR), orthogonal (OR) and generalized orthogonal (GOR) which is the best one, out of that are employed for converting different types of magnitude scales, such as surface-wave magnitude (M_S), body-wave magnitude (m_b) and local magnitude (M_L) into a single homogenized moment magnitude, M_W . The homogenized catalogue is then treated with 'runs test' to estimate p -value of 0.8421 which suggest no spurious reporting on the catalogue. The prepared catalogue has also been declustered using standard procedure. Furthermore, the magnitude of completeness for space and time with 90% confidence level has been achieved. The seismicity parameters, namely magnitude of completeness M_C , a -value and b -value are found to be 4.6, 7.50 and $0.95(\pm 0.023)$, respectively. The observed low b -value implies that the study region is tectonically very active with the presence of asperity.

ARTICLE HISTORY


Received 23 December 2016
Accepted 2 June 2017

KEYWORDS

Generalized orthogonal regression; homogenization; M_C ; a -value and b -value; Northeast India

Introduction

The Northeast region of India is seismically very active and its seismicity is primarily attributed to the Indian-Asian plates collision in the north and Indian-Sunda plates interaction in the Indo-Burmese arc in the east (Bilham and England 2001; Kayal et al. 2012). The mechanical deformations due to these interactions resulted in the formation of the most seismically active Himalayan thrust faults in the north, Arakan-Yoma, Naga Hills and Tripura folded belt in the east and also the uplift of Shillong plateau in the zone-III (Thingbaijam et al. 2008). As per the seismic zonation map of India, the region lies in zone-V, the highest seismic active zone (Bureau of Indian Standards 2002). Bhatia et al. (1999) estimated the peak ground acceleration (PGA) which was found within the range, 0.35–0.45g for the Global Seismic Hazard Assessment Programme. Moreover, Das et al. (2016) also estimated the mean PGA value for 50%, 20%, 10%, 2% and 0.5% probabilities of exceedance in 50 years, corresponding to return periods of 100, 225, 475, 2475 and 10,000 years respectively and found to be 0.19, 0.251, 0.323, 0.5 and 0.68 g in this region. Several large to great earthquakes namely, 12 June 1897 Shillong ($M_W = 8.1$), 15 August 1950 Assam earthquake

CONTACT P. N. S. Roy  roy.pns.agp@ismdhanbad.ac.in; pns_may1@yahoo.com



 Supplemental data for this article can be accessed at  <https://doi.org/10.1080/19475705.2017.1345794>.

Table 1. List of some notable earthquakes 1869, 1897, etc., in the Northeast Indian region.

Place	Date	Latitude	Longitude	Magnitude	Description
Cachar earthquake	10 January 1869	24.66	92.85	M_W -7.3	Damaging in the region from Dhubri to east of Imphal and between Nowgong and Silchar
Shillong earthquake	12 June 1897	26.00	91.00	M_W - 8.1	Damaged every stone house, 13 deaths. Damages were observed in Umananda Island temple and railway lines
Dhubri earthquake	3 July 1930	25.93	90.18	M_W -7.1	In Dhubri area, damages of the buildings. No fatalities
Assam earthquake	29 July 1947	28.50	94.00	M_W -7.3	Cracks in walls at Guwahati area. Failure of electricity observed
Assam earthquake	15 August 1950	26.6	96.5	M_W - 8.6	1500 people were killed and the drainage affected
Near Moirang, Southern Manipur	1 July 1957	24.40	93.80	M_W - 7.2	10,000 people died
East of Imphal (Indo-Myanmar Border region)	6 August 1988	25.14	95.12	M_W -7.2	Three people killed and 12 injured and considerable damage and landslides in the Guwahati–Sibsagar–Imphal region
Sikkim earthquake	18 September 2015	27.72	88.06	M_W - 6.9	111 people were killed. Most of the deaths occurred in Sikkim. Several buildings collapsed in Gangtok
Manipur earthquake	3 January 2016	24.83	93.65	M_W - 6.8	11 people killed, 200 others injured and buildings damages

($M_W = 8.6$) and 6 August 1988 Manipur–Myanmar earthquake ($M_W = 7.2$) which collectively claimed thousands of lives and devastated poor structured buildings have occurred in this region (Table 1, Oldham 1899; Bilham 2004). Additionally, several damaging earthquakes having magnitude ~ 7 , although with their relatively low recurrence intervals, made this region seismically prone and vulnerable to hazard. Hence, using a reliable and accurate catalogue, quantification of seismicity parameters are essential and necessary for developing a probabilistic and deterministic hazard map for safety of millions of lives living in and around the region.

Usually earthquake catalogue comprises of many magnitude scales such as M_L , m_b and M_S based on the recordings of their wave types of the earthquakes. M_L , commonly known as Richter local magnitude, is found to be widely used magnitude scale in the world. However, this scale gives inaccurate magnitude for the large earthquakes due to its saturation above magnitude 6 (Hutton and Boore 1987). Based on body waves, body wave magnitude, m_b is established to overcome the saturation problem but the scale fails for the 6–8 magnitude (Gutenberg and Richter 1956). Another magnitude scale known as surface-wave magnitude scale, M_S was introduced by Gutenberg and Richter (1956) for resolving the same saturation issue. But still, M_S tends to saturate above magnitude 8 and hence another alternative magnitude scale based on seismic energy was required to be introduced. The saturation of these magnitude scales is completely dependent on the amplitudes of their wave types. As such, Kanamori (1977) proposed another magnitude scale, moment magnitude scale (M_W), which is based on seismic energy in order to measure for any larger earthquakes without any saturation. Hence, it can be concluded that M_W is recognized as a stable scale for measuring large earthquakes (Lay and Wallace 1995). However, the presence of inhomogeneities in the magnitude scale due to various magnitudes should be corrected before robust estimation of any statistical analyses (Chingtham et al. 2014). Therefore, homogenization of different magnitude scales into a single magnitude scale by using different regression techniques is a basic requirement (Gutenberg and Richter 1956; Bath 1968; Chingtham et al. 2016). By doing so, one magnitude scale can be converted into other magnitude scale by establishing the empirical relationships between the correlated events (Marshall 1970; Gibowicz 1972; Das and Wason 2010; Nguyen et al. 2011). But, the conversion of one magnitude scale into another magnitude scale is accepted only when the estimated standard deviations associated with the regression parameters are negligibly low (Stromeyer et al. 2004; Joshi and Sharma 2006; Thingbaijam et al. 2008; Das et al. 2011). Several authors (Thingbaijam et al. 2008; Ristau 2009; Yadav et al. 2009; Mousavi-Bafrouei et al. 2014; Chingtham et al. 2015;

Chingtham et al. (2016) have used least square (ISR), orthogonal regression (OR) and generalized orthogonal regression (GOR) techniques for converting the different magnitude scales into a single magnitude scale in different tectonic settings of the world. During the period 1905–2007, Thingbaijam et al. (2008) and Thingbaijam (2009) utilized the International Seismological Centre (ISC) and Global Centroid Moment Tensor Solution (GCMT) databases to compile the homogenized earthquake catalogue (M_W) by using GOR technique in Northeast region of India. For the same region using ISC and GCMT, Yadav et al. (2009) converted the different magnitude scales into single seismic moment, M_W by adopting SR technique during the period 1905–2007. However, Das et al. (2012) used the period of 1978–2006 for events in ISC, GCMT and National Earthquake Information Centre (NEIC) catalogues for the conversion of m_b and M_S magnitudes into the unified moment magnitude, M_W by adopting orthogonal least square regression (OSR) relationships in Northeast India. In northwest Himalaya and its surrounding region, Chingtham et al. (2014) adopted GOR technique to convert different magnitude scales into M_W for the India Meteorological Network (IMD) seismological network covering a period from 1 June 1998 to 30 June 2011 in the Northwest Himalaya and its surrounding region. Empirical relationships among M_L , teleseismic m_b , M_W have been firmly established though SR, ISR and GOR techniques for homogenization of catalogue in New Zealand by using GeoNET and GCMT catalogue during the period 1977–2008 (Ristau 2009). Mousavi-Bafrouei et al. (2014) used the regression relations such as SR, ISR, OR and GOR for converting different magnitude scales into M_W for Iran and its adjacent regions by using historical, ISC and NEIC catalogues since fourth century BC until 2012.

In this study, we have applied the GOR technique for converting different magnitude scales such as M_L , m_b and M_S into M_W by using the ISC and GCMT catalogues during the period 1 January 1900 to 31 April 2016. Subsequently, we have also considered the historical and modern earthquake catalogues compiled by several authors/agencies in the Northeast region in order to not miss a single event in the homogenized catalogue. The known or published M_W is finally used to replace the compiled M_W in the catalogue. The reason behind the conversion of different magnitude scales into single moment magnitude M_W lies on the fact that it remains unsaturated over all the magnitude scale with accuracy found to be two or three times higher than other magnitude types. Uhrhammer (1986) established the declustered technique for removing the foreshocks and aftershocks by applying the space-time window around the mainshocks from the homogenized moment magnitude M_W . Later on, for this study region we have calculated the magnitude of completeness in terms of space and time for frequency magnitude distribution (FMD) at 90% confidence level, the primary parameter for analysis of a -value and b -value for our study region. Wiemer and Wyss (2000) developed the maximum curvature method for estimation of the magnitude of completeness M_C . A graphical technique well known was proposed as Mulargia and Tinti (1985) the visual cumulative method to check the stable and significant recording of events. Then, the magnitude of completeness, M_C and its associated parameters a -value and b -value have been estimated from this declustered catalogue using maximum curvature method developed by Wiemer and Wyss (2000). Finally, we have also examined the plot between the cumulative number of earthquake and hour of the day to investigate the extraneous recordings obtained from the possible quarry blast.

Seismotectonic setting of the region

The study region, bounded by the latitude 21°N–30°N and longitude 87°E–98°E, is surrounded by the EW trending Himalaya belt to the north, NS trending Arakan-Yoma belt to the east and the Bengal basin to the south (Figure 1). The EW trending Himalaya belt is associated with the collision between the Indian and the Eurasian plates while the Arakan-Yoma belt is associated with the interaction of Indian plate beneath the Burma plate (Dasgupta et al. 2000). Notably, the alluvium of Brahmaputra River and the Shillong-Mikir plateau that are observed in the study region are found to be sandwiched between these tectonic belts (Nandy 2001). The tectonics of the study region can also be characterized by the splays of north dipping major thrust faults formed during the Indian

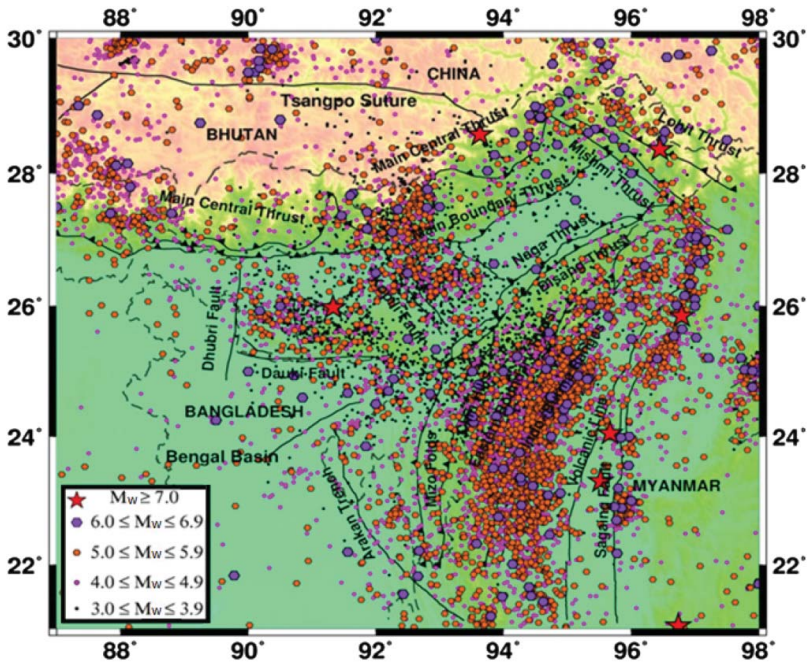


Figure 1. Seismotectonic map of Northeast India and adjoining region drawn with the declustered earthquake having minimum magnitude $M_w \geq 3$ during the period 1 January 1900 to 31 April 2016. Another seismotectonic map drawn from the catalogue before declustering has been attached as a supplementary file (S1) for comparing the spatial distributions of earthquake occurrences between the clustered and declustered earthquake catalogues.

and Eurasian plate's convergence. In this region, the major faults include the Main Central Thrust (MCT), Main Boundary Thrust (MBT), Main Frontal Thrust (MFT). Besides, the tectonic features/lineaments such as the Mishmi thrust, Lohit thrust, Po-Chu fault and Tidding suture also characterize the tectonic settings of the study region (Thingbaijam et al. 2008). It is here noteworthy to mention that the NE trending Mishmi Thrust illustrates the formation of the Eastern Himalaya due to the convergence of Indian and Eurasian plates (Thingbaijam et al. 2008).

On the basis of seismicity, geological features and orientation of the faults, the region can primarily be classified into four main seismogenic source zones, i.e. the Eastern Syntaxis (zone-I), the Arakan-Yoma Subduction Belt (zone-II), the Shillong Plateau (zone-III) and MCT and MBT of the Himalayan Frontal Thrusts (zone-IV) (Dutta 1964; Gupta et al. 1986; Roy et al. 2015). In zone-I, the NW-SE trending thrust faults such as Lohit Thrust, Mishmi Thrust and strike-slip Po-Qu fault represent the major fault systems observed in the study region. As such, the right lateral strike slip earthquake, i.e. 15 August 1950 Assam earthquake ($M_w = 8.6$) that caused irreparable damages to the mankind is associated with the NW-SE trending Po-Qu fault (Kayal 2014). Zone-II, commonly known as the Arakan-Yoma subduction zone is characterized by the subduction of Indian plate underneath the Burmese plate. Due to this, the seismicity is relatively high in comparison to other zones and subsequently, the shallow to intermediate depth earthquakes are distributed along the subducting Indian plates. From the focal mechanism of earthquakes, this zone is also found to be characterized by crustal thickening along with N-S compression. Towards the Indian plate and away from the colliding plates, there lie the Shillong plateau that can be categorized into zone-III. The Assam valley that exhibit ENE-WSW trending lies in between Shillong plateau and the eastern Himalayan tectonic belt. Besides the plateau, the zone is also characterized by several shear faults and lineament. The intraplate shallow seismicity observed in this zone is contributed by the movement/uplifting of the Shillong plateau along the major thrust/strike-slip Dauki fault (Bilham and England 2001). As such, the focal mechanisms of the observed earthquakes display significant thrust

component along with strike-slip motion. Moreover, the differential velocity of the Indian plate observed towards the northward and eastward makes this zone highly compressive stresses and distortions (Bilham and England 2001; Vernant et al. 2014). Zone-IV (the Himalayan Thrusts Zone) demarcates the boundary between the Indian and Eurasian plate continent–continent collision. Hence, the seismicity of this zone is associated with the EW striking, northward dipping MBT and MCT. In this zone, Manipur and Nagaland hills that primarily comprise the northern part of the Indo-Burma ranges merge to the Himalayan arc at the syntaxis zone. In the northeast region of India, several thrust zones are appearing, for example the Naga Thrust along the Naga Hills and the Churachandpur Mao Thrust along the Manipur hills. However, the NE-SW trending Naga thrust demarcates Assam valley zone or the Brahmaputra basin that lies on northern part of this zone. The Naga and Disang thrust are found to the southeast direction of the Kopili fault. In addition, the recognition of the Indian plate subduction zone boundary can be understood by the presence of the East Boundary Thrust (EBT) in the east direction. The appearance of Mishmi thrust in the north direction of syntaxis zone is connected to the Sagaing fault zone in the central Burma basin. The Bengal basin characterized by tertiary sediments is separated from the Precambrian shield by E-W Dauki fault and its conjugate active fault is Dapsi fault in the plateau (Baruah et al. 2012). Thus, the movement of the Shan Sagaing fault towards east direction is the primary reason of EBT zone demarcation.

Data adopted and methodology

Earthquake catalogue plays an important parameter for assessing seismic hazard of any seismotectonic regimes of the world. In this study, two international data centres such as ISC, United Kingdom (since 1964; <http://www.isc.ac.uk/search/> bulletin, last accessed June 2016), covering the period of 1 January 1900 to 31 April 2016 and the GCMT, Columbia University (<http://www.globalcmt.org>, last accessed July 2016) during the period 1 January 1976 to 31 April 2016 are adopted. However, ISC and GCMT catalogue comprises of several magnitude scales such as M_L , m_b , M_S and M_W , which are instrumentally recorded on the basis of types of magnitude waves produced during the occurrence of an earthquake. Richter (1935) proposed the local magnitude, M_L , consider as a first magnitude scale defined by the trace amplitudes of earthquakes recorded on Wood–Anderson seismographs (Lay and Wallace 1995). Depending on the radiation pattern and travel path, M_L may vary considerably from station to station. On the other hand, the body-wave magnitude scale (m_b) was introduced specifically by Gutenberg and Richter (1956) to highlight the deep-focus earthquake and long distances P-wave amplitude recorded with a period of about 1s. The surface wave magnitude scale (M_S) is measured from the ground amplitude of surface waves on standard long-period seismogram with a period of about 20s (Gutenberg 1945a, 1945b).

These magnitude scales such as M_L , m_b and M_S exhibit non-uniformity at different levels of large earthquakes and subsequently these scales fail to measure large to great earthquakes due to its saturation issues, thereby resulting magnitude error in the estimated earthquake. In the late 1970, Kanamori (1977) presented another type of magnitude scale, popularly known as moment magnitude scale, M_W . This scale is predominantly based on the scalar seismic moment, M_0 and hence valid for all size of earthquake. Theoretically, the reliability of the scale is ascribed by the fault size and the dislocation associated with the seismic moment. Hanks and Kanamori (1979) established the empirical relation between M_W and M_0 as given by

$$M_W = \frac{2}{3} \log_{10} M_0 - 6.05, \quad (1)$$

where M_0 is the scalar seismic moment in N. m.

Different magnitude scales present in the catalogue needs to be homogenized into a single consistent magnitude, M_W . As mentioned earlier, M_W is adopted because it can measure for all ranges of

earthquakes irrespective of large or small, local or teleseismic, shallow or deep epicenters. This can be accomplished by utilizing regression techniques such as SR, ISR, OR and GOR thereby establishing empirical relations M_L , m_b , M_S and M_W from the entries of the same earthquakes in the catalogues derived from the ISC and GCMT databases (e.g. Stromeyer et al. 2004; Bormann et al. 2007). SR technique is valid for the variances $\sigma_x^2 \rightarrow 0$ and $\sigma_y^2 > 0$. As such, the best fitting line drawn through this SR technique considers only the errors of the vertical distances between the experimental points (X_i, y_i) and their equivalents on the regression line (X_i, Y_i) (Bormann et al. 2007). This leads to

$$\sum_{i=1}^n [y_i - \beta x_i - \alpha]^2, \quad (2)$$

where (X_i, Y_i) and (x_i, y_i) indicate the true variable and variable affected by measurement errors respectively and α is a constant whereas β is a function of the regression slope.

ISR is similar to SR method but valid only for $\sigma_y^2 \rightarrow 0$ and $\sigma_x^2 > 0$. This indicates that the best fitting line includes only the errors of the horizontal distances between the experimental points (x_i, Y_i) and their equivalents on the regression line (X_i, Y_i) . Equation (2) can thus be modified by

$$\sum_{i=1}^n \left[x_i - \frac{y_i - \alpha}{\beta} \right]^2. \quad (3)$$

However, the GOR regression relationship technique accounts the measurement errors on both the linearly related variables. In other words, this technique simply minimizes the orthogonal residuals for both the variables obtained from their orthogonal projections on the GOR line (Das et al. 2011, 2013). On the contrary, this technique introduces biased estimations of the dependent variable, because the abscissa of the true points on the GOR line corresponding to given magnitude data pairs have been simply replaced by the abscissa of the observed error corrupted points for establishing the GOR regression relationship among the different magnitude scales (Das et al. 2012; Wason et al. 2012; Das et al. 2014b; Das et al. 2014c). Conversely, the GOR technique can be established only when a priori information on the values of the errors associated with the two variables is known and $\eta \neq 1$ (Thingbaijam et al. 2008; Yadav et al. 2009; Das et al. 2012; Chingtham et al. 2014). Here, the error variances η are estimated by following relation:

$$\eta = \sigma_x^2 / \sigma_y^2. \quad (4)$$

The general orthogonal regression estimator can thus be obtained by minimizing the given equation,

$$\sum_{i=1}^n \left[y_i - \alpha - \frac{\beta X_i}{\eta} + (x_i - X_i)^2 \right]. \quad (5)$$

OR is simply the GOR that considers the measurement errors on both variables. The only dissimilarity is that the value of η given by Equation (4) is 1. If the true η is unknown or deliberately ignored, OR gives robust result than GOR when considering the errors occurred in both types of magnitude (Castellaro et al. 2006; Castellaro and Bormann 2007; Ristau 2009). Here, GOR relationship is applied for establishing empirical relationships among the magnitude scales. The standard regression relation used for the conversion of entries, $n = 1662$ of M_L into m_b is shown by the given relation,

$$m_b = 0.9721(\pm 0.002) * M_L + 0.1065(\pm 0.008), \quad \text{for } 2.5 \geq M_L \geq 5.1 \quad (6)$$

The correlation of M_S to m_b for the entries, $n = 1798$ is observed to follow the relation:

$$m_b = 1.3278(\pm 0.003) * M_S - 1.7665(\pm 0.013), \quad \text{for } 3 \geq M_S \geq 6 \quad (7)$$

Also, the established regression relation based on the entries, $n = 69$ for converting M_S to M_W are listed below,

$$M_W = 1.1590(\pm 0.005) * M_S - 0.8168(\pm 0.0238), \quad \text{for } 3.8 \geq M_S \geq 5.8 \quad (8)$$

Moreover, the regression relation to convert M_S into M_W from the entries, $n = 13$ are depicted by the following relation:

$$M_W = 1.6019(\pm 0.179) * M_S - 3.2919(\pm 1.134), \quad \text{for } 5.9 \geq M_S \geq 7.2 \quad (9)$$

Finally, the obtained regression relation for converting m_b to M_W from the entries, $n = 255$ are shown by the given relation,

$$M_W = 1.0312(\pm 0.007) * m_b - 0.0123(\pm 0.036) \quad \text{for } 4.3 \geq m_b \geq 6.2 \quad (10)$$

The details of the regression equations among different magnitude scales obtained from SR, ISR, OR and GOR are given in [Table 2](#). ‘Runs test’ is then treated to the homogenized catalogue obtained from these regression equations for checking the spurious reporting in the catalogue. Finally, the different empirical based statistical methods have been adopted by several authors/scientists ([Utsu 1969](#); [Gardner and Knopoff 1974](#); [Reasenberg 1985](#); [Uhrhammer 1986](#)) for filtering the dependent events, i.e. foreshocks and aftershocks, thereby applying the space-time window around the mainshock. The basic differences among these methods can be primarily attributed to the size of the window, duration of the sequences after the mainshock and finally the magnitude of the earthquakes. Here, the method given by [Uhrhammer \(1986\)](#) has been utilized to clean the foreshocks and

Table 2. Illustration of the regression parameters-intercept α , slope β , ratio of error variances $\eta = \sigma_x^2/\sigma_y^2$, and number of events, n of various regression technique.

$x-y$	Regression	α	β	η	n
M_L-m_b	GOR	0.1065(± 0.008)	0.9721(± 0.002)	0.52	1662
	OR	0.9079(± 0.194)	0.7559(± 0.052)		
	SR	1.9381	0.4780		
	ISR	1.9429	1.5250		
m_b-M_S	GOR	-1.7665(± 0.013)	1.3278(± 0.003)	0.67	1798
	OR	-1.3776(± 0.087)	1.2319(± 0.021)		
	SR	0.2983	0.8188		
	ISR	3.0390	1.6414		
m_b-M_W	GOR	-0.0123(± 0.036)	1.0312(± 0.007)	0.82	255
	OR	0.1115(± 0.231)	1.0072(± 0.045)		
	SR	1.1179	0.8119		
	ISR	1.1191	1.2461		
M_L-M_W	GOR	2.2624(± 0.174)	0.6600(± 0.038)	0.29	26
	OR	3.2271(± 1.584)	0.4502(± 0.344)		
	SR	3.6579	0.3564		
	ISR	-0.5421	1.0344		
M_S-M_W ($3.8 \geq M_S \geq 5.8$)	GOR	-0.8168(± 0.0238)	1.1590(± 0.005)	1.27	69
	OR	-0.8291(± 0.272)	1.1616(± 0.058)		
	SR	-0.7122	1.1367		
	ISR	0.9176	1.1805		
M_S-M_W ($5.9 \geq M_S \geq 7.2$)	GOR	-3.2919 (± 1.134)	1.6019(± 0.179)	1.37	13
	OR	-3.3593(± 2.811)	1.6125(± 0.445)		
	SR	-3.0576	1.5647		
	ISR	3.4789	1.6315		

aftershocks from the mainshocks. Later, the magnitude of completeness (M_C) that defined the minimum magnitude at which the power law fit as best fit for FMD is obtained at 90% confidence level is calculated for the study region. This is an essential parameter for estimating a -value and b -value for hazard assessment in any tectonic regimes. In this study, 'maximum curvature' method given by Wiemer and Wyss (2000) is adopted to estimate M_C . This involves the finding of maximum curvature from the graph constructed in between the magnitude and the logarithm of the cumulative numbers of events above this magnitude. Moreover, the information of the time of completeness for different magnitude range is essential for quantifying the seismicity parameters. A well-known graphical technique, i.e. visual cumulative method established by Mulargia and Tinti (1985), is used here for calculating the time period of catalogue completeness. The technique comprises of fitting a straight line to the slope of the data observed in the graph that are constructed between time and cumulative number of events for a particular magnitude range. Therefore, the completeness of small to moderate earthquakes is found within instrumental period whereas the completeness of large earthquakes can be traced back to pre-instrumental era (Yadav et al. 2009).

Results and discussions

In this study, a homogenized earthquake catalogue pertaining to Northeast India and its adjoining region (lat. 21° – 30° N and long. 87° – 98° E) has been compiled by using different regression techniques during the time period 1 January 1900 to 31 April 2016. For this purpose, 14,031 events, having magnitude on different scales such as M_L , m_b and M_S have been assessed from ISC database. For these magnitude scales, the regression techniques such as SR, ISR, OR and GOR are adopted to establish the correlation relationships in between M_S - m_b , m_b - M_L , M_S - M_L , M_W - M_L , M_W - m_b and M_W - M_S as shown by Figure 2(a–f) and Table 2. From Figure 2(b,c), we have observed that both the correlations of m_b - M_L and M_S - M_L are found to be valid up to M_L of 5.2. Furthermore, the relationship between m_b - M_S is found to be valid for M_S having maximum value of 6.3 as shown in Figure 2(a). We have also segregated the range of M_S into two parts (i.e. $3.8 \geq M_S \geq 5.8$; $5.9 \geq M_W \geq 7.2$) based on the linearity of observed data for converting M_S into M_W . Similar observations have also been found in their established regression relations for converting M_S into M_W by several authors/scientists (Scordilis 2006; Das et al. 2014a). Beyond these magnitudes, the magnitude scales will saturate and subsequently leads to mild incoherency between the linear regressions. Notably, the η value of the GOR obtained through the iterative search and that correspond to the lower standard deviation of β is found to be considerably low, i.e. below 1 for all the correlations between different magnitude scales. This simply implies that the β associated with OR is found to be affinity towards β associated with SR for all the regression relationships except the correlation M_S - M_L . It is also observed that the relations derived from this GOR technique have significantly lower errors in their regression parameters than the corresponding relations established from other techniques as shown in Table 2 (Thingbaijam et al. 2008; Yadav et al. 2009). Consequently, as mentioned earlier, the equation obtained through this technique gives comparably low standard deviation for β (Table 2) and hence only GOR equations are adopted for conversion process. Also, as compared to the corresponding SR relation established by Scordilis (2006), this GOR technique is also associated with lower uncertainties. These results are intriguing and found unison with the understandings of Castellaro and Bormann (2007). It is also noteworthy to mention here that the GOR regression relations derived (Equations (6)–(10)) are found to be consistent with the existing regression equations established by several authors in this region (Thingbaijam et al. 2008; Yadav et al. 2009; Das et al. 2011; Das et al. 2012; Das et al. 2014a). By using this regression technique, we can easily convert one magnitude scale into another scale through the equation, $y = \alpha + \beta.x$. However, any magnitude scale can be converted into another scale through connection of the entries in other catalogues on one–one correspondence, if the correlations cannot be established directly between the magnitude scales. In this study, M_L and M_S entries found in the catalogue have been converted and scaled into m_b through Equations (6) and (7), respectively. Finally, the total magnitude scale m_b obtained is scaled into

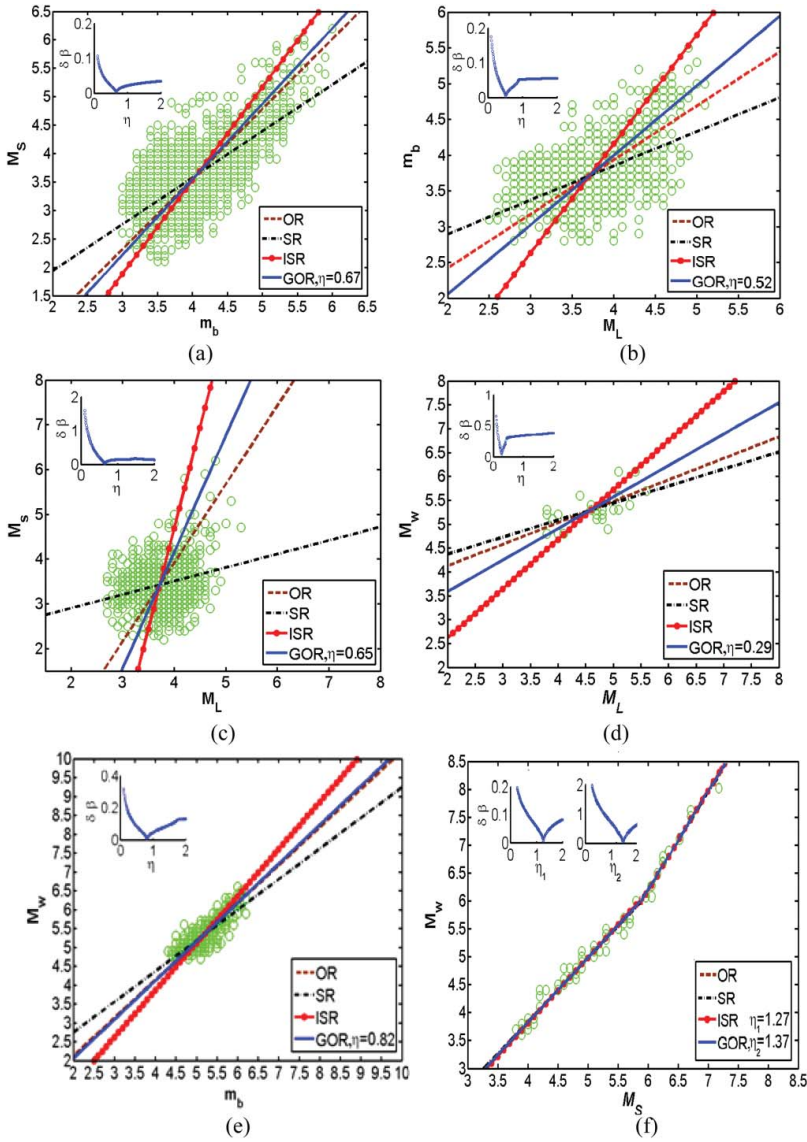


Figure 2. Regression relation between M_S - m_b , m_b - M_L , M_S - M_L , M_W - M_L , M_W - m_b and M_W - M_S through the SR, ISR, OR, GOR technique shown in Figure 2(a-f) for the Northeast region of India.

moment magnitude scale M_W by establishing the relationship between M_W - m_b (Equation (10)), using GOR technique. For such conversion process, we have utilized the M_W entries recorded by GCMT in the study region during the period 1 January 1976 to 31 April 2016. However, the correlation between M_W - m_b is valid up to m_b of 6.3 (Figure 2(e)) and hence beyond this value of m_b will contribute errors in the derived Equation (10) due to its saturation. Similar to Equation (8), the η value of the GOR is found to be low, thereby exhibiting β associated with OR affinity towards β associated with SR. However, the associated errors with the variables are found to be high in the regression equation for converting M_S into M_W and hence M_S - M_W regression relation is not employed during the homogenization process (Equations (8) and (9)). Then, the large M_W entries documented in different literatures have been used for replacing the M_W entries found in the homogenized catalogue. Here, we have also observed that the absolute average difference between

our homogenized catalogue (M_W) and the other existing catalogues (M_W) differs by 0.4 m.u. and this can be primarily correlated with the adopted earthquake databases and the duration of the catalogue. For this study region, Thingbaijam et al. (2008) established the empirical relationships among the magnitude scales, adopted from ISC and GCMT for scaling m_b and M_S into M_W during the period, 1906–2006. Yadav et al. (2009) compiled the homogenization earthquake catalogue in M_W with the help of earthquake databases (e.g. India Meteorological Department (IMD); Geological Survey of India (GSI); NEIC of USGS; ISC) spanning the period 1846 to 1995 for the same study region. The basic difference between these two authors lies on the fact that Thingbaijam et al. (2008) utilized GOR technique while Yadav et al. (2009) adopted OR technique for the homogenization process. Moreover, Das et al. (2011) compiled a unified moment magnitude in M_W by utilizing orthogonal standard regression (OSR), while Baruah et al. (2012) established empirical relation between M_L and M_W by using linear regression analysis (OSR), thereby classifying the Northeast India into different tectonic zones. Several authors (e.g. Thingbaijam et al. 2008; Baruah et al. 2012) from their studies revealed that M_L and M_W exhibit almost similar magnitude values, which is also corroborated by several researchers in different tectonic regimes of the world (Ristau et al. 2005; Deichmann 2006). However, Yadav et al. (2009) strongly argued this conclusion by mentioning that the similarity between M_L and M_W holds true only for small magnitudes not for large magnitudes. During the study period, the M_W homogenized earthquake catalogue consists of 18,477 earthquakes with magnitude $M_W \geq 2.5$. However, this earthquake catalogue comprises of several dependent shocks (i.e. foreshocks and aftershocks) as depicted in Figure 3. A declustering technique adopted by Uhrhammer (1986) is utilized to remove the foreshocks and aftershocks from the mainshocks. Therefore, this method removes 41.1% of dependent events (foreshocks and aftershocks) from the 12,223 clusters formed in the entire catalogue (Figure 4). Moreover, Yadav et al. (2009) and Das et al. (2011) adopted the Uhrhammer (1986) method for declustering the homogenized catalogue in this region. From this declustered catalogue, the value of M_C is estimated to be 4.6 from the FMD of earthquakes as shown in Figure 5. While considering all the earthquakes above this M_C value, the associated parameters a -value and b -value are estimated from the ‘maximum curvature’ method given by Wiemer and Wyss (2000). Here, a -value and b -value are found be 7.50 and $0.95(\pm 0.023)$ respectively in this study region (Figure 6). The high a -value in the study region implies that the hazard level in terms of seismicity is predominantly high with observed large earthquakes occurring in the region. Moreover, the low b -value of $0.95(\pm 0.023)$ revealed the seismogenesis of the study region. Comparison to global b -value of 1, the estimated b -values confirmed that the study region comprises of several asperity zones with highly build up differential stress (Wiemer and Katsumata 1999; Wiemer and Wyss 2002). Furthermore, Nuannin et al. (2005) also highlighted that the induced low b -value are primarily due to the observed large earthquake occurrences in the region.

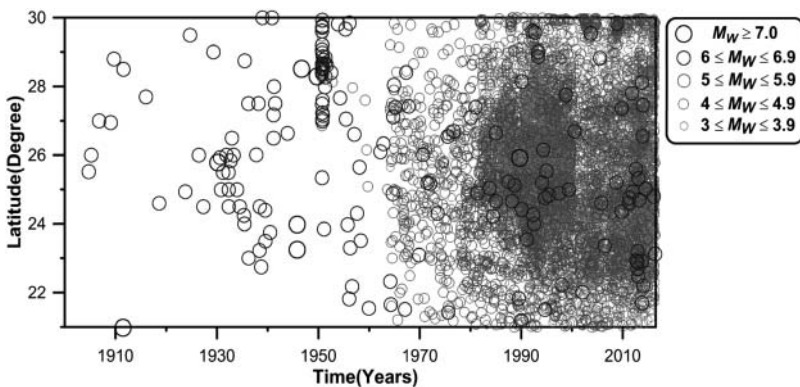


Figure 3. Time-latitude plot of the earthquakes having minimum magnitude, $M_W \geq 3$ before the declustering of catalogue in the study region during the period 1 January 1900 to 31 April 2016.

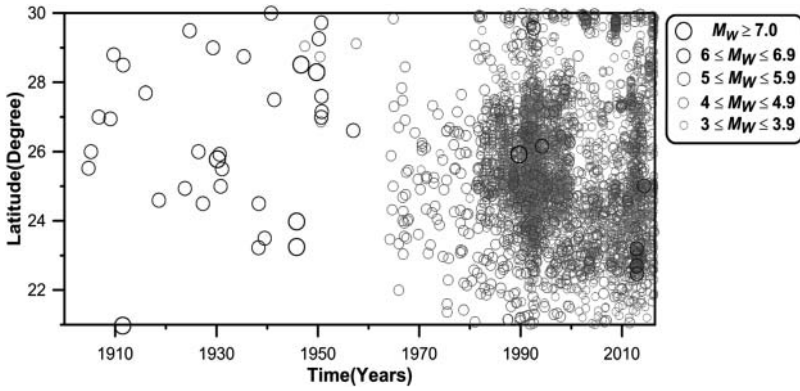


Figure 4. Time-latitude plot of the earthquakes having minimum magnitude, $M_W \geq 3$ after the declustering of catalogue in the study region during the period 1 January 1900 to 31 April 2016. The method of Uhrhammer (1986) is applied to the earthquake events for declustering the foreshocks and aftershocks (dependent events) using magnitude-dependent space and time windows.

The results for these parameters have been found similar with those findings of several researchers in Northeast India (Thingbaijam et al. 2008; Yadav et al. 2009). In addition; the completeness analysis with time has been checked by using visual cumulative method given by Mulargia and Tinti (1985). From such studies, we have observed that the magnitudes $M_W \geq 3.0$, $M_W \geq 4.0$, $M_W \geq 5.0$ and $M_W \geq 6.0$ have been found complete starting from 1902, 1963, 1986 and 1993, respectively. The sole responsible for this improvement in the M_C values is the increased number of networks along with the increased azimuthal coverage of these networks in the study region. Thingbaijam et al. (2008) found that the completeness with respect to time has been confirmed for magnitudes $M_W \geq 4.0$, $M_W \geq 4.5$, $M_W \geq 5.0$ and $M_W \geq 5.7$ since 1964, 1963, 1921 and 1924, respectively. Whereas, Yadav et al. (2009) exhibited that the recordings for the magnitudes, $M_W \geq 4.0$, $M_W \geq 4.5$, $M_W \geq 5.0$, $M_W \geq 5.5$ and $M_W \geq 6.0$ are stable and complete starting from the years 1987, 1975, 1963, 1921 and 1914, respectively. However, our result for this completeness of magnitude with time approaches to the values obtained by Yadav et al. (2009). Later, the plot in between the number of events and hour of the day exhibit that our final catalogue does not contain any spurious recordings resulting from bomb blasting, quarry blasts etc. (Wiemer and Baer 2000). This has also been confirmed from the ‘runs test’ that check the random distribution above and below the average number of events per hour, i.e. 153 as shown in Figure 7. The p -value of 0.8421, as obtained from this test

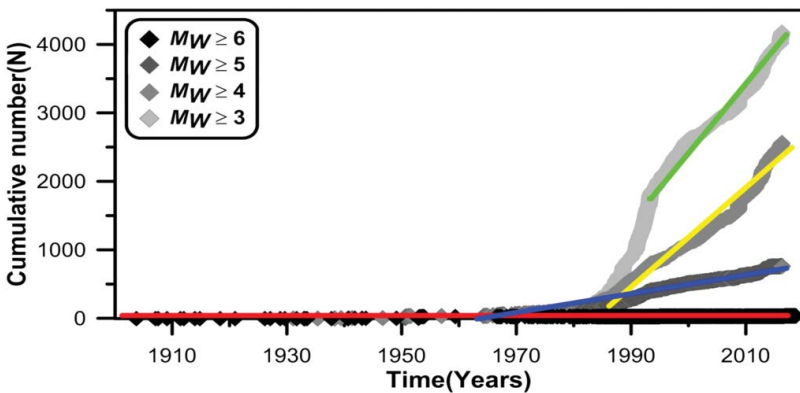


Figure 5. Graph showing the analysis of completeness period of the earthquake by plotting between time (years) and cumulative numbers of events for various range of earthquake magnitudes.

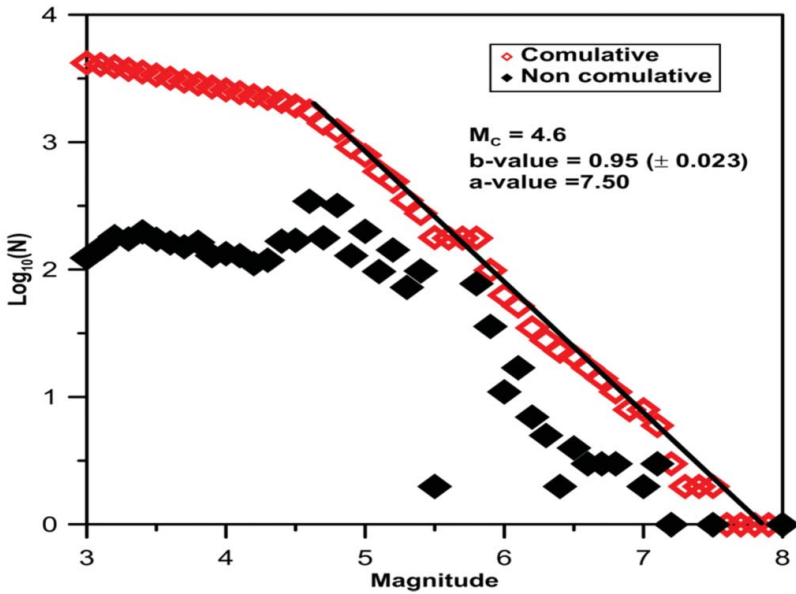


Figure 6. Plot of frequency-magnitude distribution relationship for Northeast India and its adjoining region. The magnitude of completeness is estimated to be 4.6 with b -value of 0.95 (± 0.023).

suggests that the hypothesis can be considerably non-rejected. This improved and upgraded homogenized earthquake catalogue can provide the strong foundation for seismic hazard assessment and other related seismological studies in this highly tectonic seismic regime.

Bayliss and Burton (2007) used the Gutenberg–Richter cumulative frequency-magnitude method to analyse the magnitude distribution for Bulgaria and the surrounding Balkan area. The authors have estimated the seismicity parameters, M_C , a -value and b -value, and found to be 4.6, 4.62 (± 0.18) and 0.820 (± 0.03), respectively, for his study region. Using EMR method, Pailoplee (2014) calculated the M_C , a -value and b -value as 3.8, 4.01 0.54(± 0.02) for Thailand region during the period of 1998–2009. Moreover, Panzera et al. (2015) followed the maximum curvature method (Wiemer and Wyss 2000) to estimate the M_C and b -value while maximum likelihood method is adopted by Utsu (1965) to estimate the b -value. Through their studies, we can conclude that no

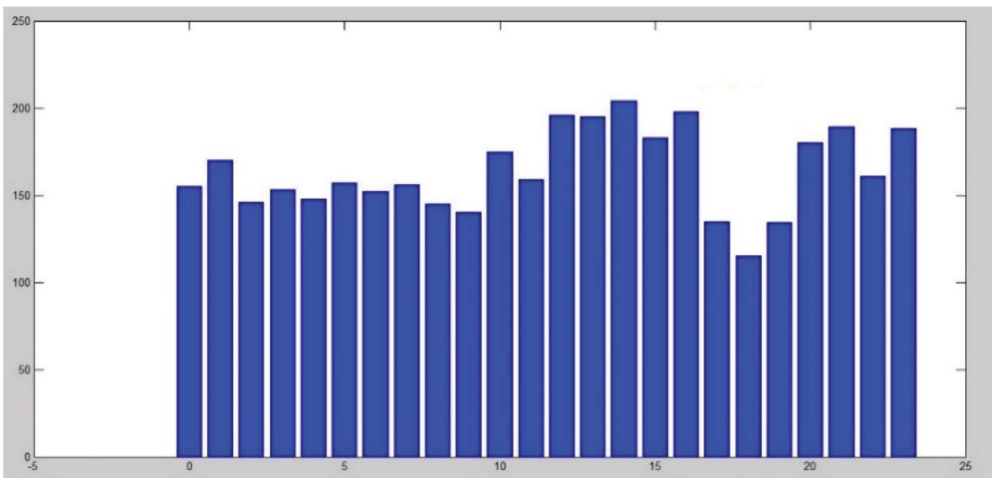


Figure 7. Plot of the cumulative number of events against hour of the day in the study region.

significant differences have been observed in the adopted methodologies for estimating the M_C , a -value and b -value.

Conclusions

In this study, the raw events that are documented by the ISC and GCMT databases during the period 1 January 1900 to 31 April 2016 and 1 January 1976 to 31 April 2016, are accessed to convert the different magnitude scales such as M_L , m_b and M_S into a single moment magnitude, M_W . For this purpose, the GOR approach has been utilized to establish the empirical relations among the magnitude scales (M_L , m_b and M_S). The reason behind the adoption of GOR technique lies on the fact that the technique considers both the uncertainties associated with the dependent and independent magnitudes, thereby reducing the errors in the regression process. After the homogenization of earthquake catalogue in M_W , the known or published M_W documented in several literatures are used to replace the existing M_W in the catalogue. Later, the catalogue is treated with declustering method for removing the 41.1% of dependent events (foreshocks and aftershocks) from the 12,333 clusters formed in the entire catalogue. Using the maximum likelihood method, the M_C , a -value and b -value are estimated to be 4.6, 7.50 and $0.95(\pm 0.023)$, respectively. The completeness with respect to time has also been checked by simply visual cumulative method and hence the magnitudes $M_W \geq 3.0$, $M_W \geq 4.0$, $M_W \geq 5.0$ and $M_W \geq 6.0$ are found to be complete and stable since 1993, 1986, 1963 and 1902, respectively. The p-value of 0.8421 obtained from the 'runs test' reveal that our final catalogue is found to be uncontaminated and did not contain any extraneous recordings. This can also be verified by the random distribution above and below the average number of events per hour, i.e. 153. Hence, the prepared upgraded and homogenized earthquake catalogue in M_W can significantly reflect the true values of seismicity parameters for assessing the seismicity hazard level in this earthquake prone region.

Acknowledgments

The authors are very thankful to Dr V. K. Gahalaut, director, National Centre for Seismology, New Delhi, for his needful support to complete this research work. The authors are also grateful to the Ministry of Earth Science (NCS, MoES) for providing the excellent facility to complete my research work. The authors are acknowledging Prof. R. P. Singh, editor-in chief, and anonymous reviewers for their valuable comments and suggestions in the original statement of manuscript. The authors are very thankful to Indian Institute of Technology (Indian School of Mines), Dhanbad, for providing financial support during this work. The authors acknowledge Paul Wessel and the University of Hawaii for general mapping tools (Wessel and Smith 1998). The authors also gratefully acknowledge the Ministry of Earth Science, Government of India for partly sponsoring this work (project number: MOES/P.O. (Seismo)/1(148)/2012).

Disclosure statement

No potential conflict of interest was reported by the authors.

Funding

This work was supported by the Ministry of Earth Sciences [grant number MOES/P.O. (Seismo)/1(148)/2012].

References

- Baruah S, Baruah S, Bora PK, Duarah R, Kalita A, Biswas R, Gogoi N, Kayal JR. 2012. Moment magnitude (M_W) and local magnitude (M_L) relationship for earthquakes in Northeast India. *Pure Appl Geophys.* 169:1977–1988.
- Bath M. 1968. Handbook on earthquake magnitude determination. 2nd ed. Uppsala: Sweden Seismological Institute.
- Bayliss TJ, Burton PW. 2007. A new earthquake catalogue for Bulgaria and the conterminous Balkan high hazard region. *Nat Hazards Earth Syst Sci.* 7:345–359.

- Bhatia SC, Kumar MR, Gupta HK. 1999. A probabilistic hazard map of India and adjoining regions. *Ann Geofis.* 42:1153–1164.
- Bilham R. 2004. Earthquakes in India and the Himalaya: tectonics, geodesy and history. *Ann Geophys.* 47:839–858.
- Bilham R, England P. 2001. Plateau pop-up during the great 1897 Assam earthquake. *Nature.* 410:806–809.
- BIS IS 1893–2002. 2002. Indian standard criteria for earthquake resistant design of structures, part 1 – general provision and buildings. New Delhi: Bureau of Indian Standard.
- Bormann P, Liu R, Ren X, Gutdeutsch R, Kaiser D, Castellaro S. 2007. Chinese national network magnitudes, their relation to NEIC magnitudes, and recommendations for new IASPEI magnitude standards. *Bull Seismol Soc Am.* 97:114–127.
- Castellaro S, Bormann P. 2007. Performance of different regression procedures on the magnitude conversion problem. *Bull Seismol Soc Am.* 97:1167–1175.
- Castellaro S, Mulargia F, Kagan YY. 2006. Regression problems for magnitudes. *Geophys J Int.* 165:913–930.
- Chingtham P, Chopra S, Baskoutas I, Bansal BK. 2014. An assessment of seismicity parameters in northwest Himalaya and adjoining regions. *Nat Hazards.* 71:1599–1616.
- Chingtham P, Sharma B, Chopra S, Roy PNS. 2016. Statistical analysis of aftershock sequences related with two major Nepal earthquakes: April 25, 2015, M_W 7.8 and May 12, 2015, M_W 7.2. *Ann Geophys.* 59:S0540–16.
- Chingtham P, Yadav RBS, Chopra S, Yadav AK, Gupta AK, Roy PNS. 2015. Time-dependent seismicity analysis in the Northwest Himalaya and its adjoining regions. *Nat Hazards.* 80:1783–1800.
- Das R, Sharma ML, Wason HR. 2016. Probabilistic seismic hazard assessment for Northeast India region. *Pure Appl Geophys.* 173:2653–2670.
- Das R, Wason HR. 2010. Comment on “A homogeneous and complete earthquake catalog for Northeast India and the adjoining region”. *Seism Res Lett.* 81:232–234.
- Das R, Wason HR, Sharma ML. 2011. Global regression relations for conversion of surface wave and body wave magnitudes to moment magnitude. *Nat Hazards.* 59:801–810.
- Das R, Wason HR, Sharma ML. 2012. Magnitude conversion to unified moment magnitude using orthogonal regression relation. *J Earth Sci.* 50:44–51.
- Das R, Wason HR, Sharma ML. 2013. General orthogonal regression relations between body-wave and moment magnitudes. *Seismol Res Lett.* 84:219–224.
- Das R, Wason HR, Sharma ML. 2014a. Unbiased estimation of moment magnitude from body and surface-wave magnitudes. *Bull Seismol Soc Am.* 104:1802–1811.
- Das R, Wason HR, Sharma ML. 2014b. Reply to “Comment on ‘general orthogonal regression relation between body-wave and moment magnitude’ by Ranjit Das, HR Wason and ML Sharma” by Paolo Gasperini and Barbara Lolli. *Seismol Res Lett.* 85:352–353.
- Das R, Wason HR, Sharma ML. 2014c. Reply to “Comment on ‘magnitude conversion problem using general orthogonal regression’ by HR Wason, R Das and ML Sharma” by P Gasperini and B Lolli. *Geophys J Int.* 196:628–631.
- Dasgupta S, Pande P, Ganguly D, Iqbal Z, Sanyal K, Venaktraman NV, Dasgupta S, Sural B, Harendranath L, Mazumadar K, et al. 2000. Seismotectonic atlas of India and its environs. Calcutta: Geological Survey of India.
- Deichmann N. 2006. Local magnitude, a moment revisited. *Bull Seismol Soc Am.* 96:1267–1277.
- Dutta TK. 1964. Seismicity of Assam – zones of tectonic activity. *Bull Natl Geophys Res Inst.* 2:152–163.
- Gardner JK, Knopoff L. 1974. Is the sequence of earthquakes in southern California, with aftershocks removed, Poissonian? *Bull Seismol Soc Am.* 64:1363–1367.
- Gibowicz SJ. 1972. The relationship between teleseismic body-wave magnitude m and local magnitude ML from New Zealand earthquakes. *Bull Seismol Soc Am.* 62:1–11.
- Gupta HK, Rajendran K, Singh HN. 1986. Seismicity of Northeast India region: part I: the database. *J Geol Soc India.* 28:345–365.
- Gutenberg B. 1945a. Amplitudes of surface waves and magnitudes of shallow earthquakes. *Bull Seismol Soc Am.* 35:3–12.
- Gutenberg B. 1945b. Amplitudes of P, PP, and S and magnitude of shallow earthquakes. *Bull Seismol Soc Am.* 35:57–69.
- Gutenberg B, Richter CF. 1956. Magnitude and energy of earthquakes. *Annali di Geofisica.* 9:1–15.
- Hanks TC, Kanamori H. 1979. A moment magnitude scale. *J Geophys Res.* 84:2348–2350.
- Hutton LK, Boore DM. 1987. The M_L scale in Southern California. *Bull Seism Soc Am.* 77:2074–2094.
- Joshi GC, Sharma ML. 2006. Magnitude scale conversion relationships for Northern Indian region using bivariate analysis. 13th Symposium on Earthquake Engineering; Dec 18–20; Roorkee: Indian Institute of Technology Roorkee. p. 307–314.
- Kanamori H. 1977. The energy release in great earthquakes. *J Geophys Res.* 82:2981–2987.
- Kayal JR. 2014. Seismotectonics of the great and large earthquakes in Himalaya. *Curr Sci.* 106:188–197.
- Kayal JR, Arefiev S, Baruah S, Hazarika D, Gogoi N, Gautam JL, Baruah S, Dorbath C, Tatevossian R. 2012. Large and great earthquakes in the Shillong plateau-Assam valley area of Northeast India region: Pop-up and transverse tectonics. *Tectonophysics.* 532–535:186–192.
- Lay T, Wallace TC. 1995. Modern global seismology. New York (NY): Academic Press.

- Marshall PD. 1970. Aspects of the spectral differences between earthquakes and underground explosions. *Geophys J Royal Astron Soc.* 20:397–416.
- Mousavi-Bafrouei SH, Mirzaei N, Shabani E, Eskandari-Ghadi M. 2014. Seismic hazard zoning in Iran and estimating peak ground acceleration in provincial capitals. *J Earth Space Phys.* 40:15–38.
- Mulgaria F, Tinti S. 1985. Seismic sample areas defined from incomplete catalogs: an application to the Italian territory. *Phys Earth Planet Interi.* 40:273–300.
- Nandy DR. 2001. *Geodynamics of Northeastern India and the adjoining region.* Calcutta: ACB Publications.
- Nguyen LM, Lin TL, Wu YM, Huang BS, Chang CH, Huang WG, Le TS, Dinh VT. 2011. The first ML scale for North of Vietnam. *J Asian Earth Sci.* 40:279–286.
- Nuannin P, Kulhánek O, Persson L. 2005. Spatial and temporal *b*-value anomalies preceding the devastating off coast of NW Sumatra earthquake of December 26, 2004. *Geophys Res Lett.* 32:L11307–1–4.
- Oldham RD. 1899. Report on the great earthquake of the 12th June 1897, *Memoirs. Memoirs of the Geological Survey of India.* p. 379.
- Pailoplee S. 2014. Earthquake catalogue of the Thailand meteorological department—a commentary. *J Earthq Tsunami.* 8:1471001–1–14.
- Panzer F, Zecher JD, Vogtford KS, Eberhard DAJ. 2015. A revised earthquake catalogue for South Iceland. *Pure Appl Geophys.* 173:97–116.
- Reasenber PA. 1985. Second-order moment of central California seismicity. *J Geophys Res.* 90:5479–5495.
- Richter CF. 1935. An instrumental magnitude scale. *Bull Seismol Soc Am.* 25:1–32.
- Ristau J. 2009. Comparison of magnitude estimates for New Zealand earthquakes: moment magnitude, local magnitude, and teleseismic body-wave magnitude. *Bull Seism Soc Am.* 99:1841–1852.
- Ristau J, Rogers GC, Cassidy JF. 2005. Moment magnitude-local magnitude calibration for earthquake in western Canada. *Bull Seismol Soc Am.* 95:1994–2000.
- Roy PNS, Chowdhury S, Sarkar P, Mondal SK. 2015. Fractal study of seismicity in order to characterize the various tectonic blocks of North-east Himalaya, India. *Nat Hazard.* 77:S5–S18.
- Scordilis EM. 2006. Empirical global relations converting M_S and m_b to moment magnitude. *J Seismol.* 10:225–236.
- Stromeyer D, Grunthal G, Wahlström R. 2004. Chi-square regression for seismic strength parameter relations, and their uncertainties, with applications to an Mw based earthquake catalogue for central, northern and northwestern Europe. *J Seismol.* 8:143–153.
- Thingbaijam KKS, Chingtham P, Nath SK. 2009. Seismicity in the North-West frontier province at the Indian-Eurasian plate convergence. *Seismol Res Lett.* 80:599–608.
- Thingbaijam KKS, Nath SK, Yadav A, Raj A, Walling MY, Mohanty WK. 2008. Recent seismicity in Northeast India and its adjoining region. *J Seismol.* 12:107–123.
- Uhrhammer RA. 1986. Characteristics of northern and central California seismicity. *Earthquake Notes.* 57:21–37.
- Utsu T. 1965. A method for determining the value of bin a formula $\log n = a - bM$ showing the magnitude-frequency relation for earthquakes (with English summary). *Geophys Bull Hokkaido Uni.* 13:99–103.
- Utsu T. 1969. Aftershocks and earthquake statistics (I) some parameters which characterize an aftershock sequence and their interrelations. *J Fac Sci Hokkaido Univ Ser VII.* 3:121–195.
- Vernant P, Bilham R, Szeliga W, Drupka D, Kalita S, Bhattacharyya AK, Gaur VK, Pelgay P, Cattin R, Berthet T. 2014. Clockwise rotation of the Brahmaputra valley relative to India: tectonic convergence in the eastern Himalaya, Naga Hills, and Shillong Plateau. *J Geophys Res.* 119:6558–6571.
- Wason HR, Das R, Sharma ML. 2012. Magnitude conversion problem using general orthogonal regression. *Geophys J Int.* 190:1091–1096.
- Wessel P, Smith WHF. 1998. New improved version of the generic mapping tools released. *EOS Trans AGU.* 79:579.
- Wiemer S, Baer M. 2000. Mapping and removing quarry blast events from seismicity catalogs. *Bull Seismol Soc Am.* 90:525–530.
- Wiemer S, Katsumata K. 1999. Spatial variability of seismicity parameters in aftershock zones. *J Geophys Res.* 104:135–151.
- Wiemer S, Wyss M. 2000. Minimum magnitude of complete reporting in earthquake catalogs: examples from Alaska, the western United States and Japan. *Bull Seismol Soc Am.* 90:859–869.
- Wiemer S, Wyss M. 2002. Mapping spatial variability of the frequency-magnitude distribution of earthquakes. *Adv Geophys.* 45:259–302.
- Yadav RBS, Bormann P, Rastogi BK, Das MC, Chopra S. 2009. A homogeneous and complete earthquake catalog for Northeast India and the adjoining region. *Seismol Res Lett.* 80:609–627.